



Contents lists available at ScienceDirect

## Materials Today: Proceedings

journal homepage: [www.elsevier.com/locate/matpr](http://www.elsevier.com/locate/matpr)

## Quasi-static crushing response of square hybrid carbon/aramid tube for automotive crash box application

Ma Quanjin<sup>a,\*</sup>, M.S.A. Salim<sup>a</sup>, M.R.M. Rejab<sup>a</sup>, Otto-Ernst Bernhardt<sup>b</sup>, Ahmad Yunus Nasution<sup>a,c</sup>

<sup>a</sup> Faculty of Mechanical and Automotive Engineering Technology, University Malaysia Pahang, 26600 Pekan, Pahang, Malaysia

<sup>b</sup> University of Applied Sciences, D-67133 Karlsruhe, Germany

<sup>c</sup> Universitas Muhammadiyah Jakarta, Jl. Cempaka Putih Tengah 27, Jakarta Pusat 10510, Indonesia

### ARTICLE INFO

#### Article history:

Received 22 September 2019

Received in revised form 22 October 2019

Accepted 29 October 2019

Available online xxx

#### Keywords:

Square hybrid carbon/aramid tube

Crushing response

Crash box application

### ABSTRACT

One of the essential automotive parts is a crash box, which is essential for initial kinetic energy absorption. However, both vehicle weight and energy-absorbing performance of crash box requirements have to achieve. Recently, crash boxes made of hybrid materials have increasingly studied regarding their better crash performance and weight reduction effects compared to conventional metallic materials. Therefore, the aim of this study is to fabricate a hybrid carbon/aramid composite crash box with a hollow structure and to determine its mechanical properties under quasi-static axial compressive and tensile loading. This study shows that square hybrid carbon/aramid tubes provide an average 57.94 J energy absorption, average 0.72 kJ/kg specific energy absorption, average 62.46 kN crushing peak load, average 748.40 MPa compressive modulus and average 36.29 MPa maximum stress under quasi-static compressive loading. It is suggested that a square hybrid carbon/aramid tube could have the promising potential to replace aluminium or metallic structure to use as an automotive crash box for lightweight applications.

© 2019 Elsevier Ltd. All rights reserved.

Selection and peer-review under responsibility of the scientific committee of the First International conference on Advanced Lightweight Materials and Structures.

### 1. Introduction

Nowadays, the automotive manufacturing industry is increasingly concerned on advancing safety features and related performance with lightweight materials such as aluminium and composites. The crash box is designed to be placed between bumper and side rails in the automotive vehicle application to protect passengers' safety and vehicle components by absorbing initial kinetic energy in case of a frontal collision [1]. The performance of the crash box can be evaluated according to the Research Council for Automotive Repairs (RCAR) regulations [2], which is generally used for frontal collision and rear protective devices. The automotive crash box is commonly used as aluminium and composite material to improve the energy-absorbing performance while reducing its weight and production costs.

Numerous researchers have determined mechanical properties and crashworthiness characteristics of different cross-section shapes of the crash box using both experimental and numerical methods [3–6]. To improve stiffness and energy-absorbing charac-

teristics, the weight of related components, fiber reinforced laminates have broadly used for the optimization of super-lightweight vehicle frame structures [7]. Hamidreza zarie et al. have studied the delamination of layers for crash boxes fabricated using glass/polyamid woven fiber [8]. Ghasemnejad et al. have investigated the effect of interlaminar fracture toughness of glass fiber/epoxy and found that energy absorption capacity was increased due to higher interlaminar fracture toughness [4]. Ghasemnejad et al. have studied the failure type of hybrid composite box, which was examined regarding the delamination of composite material results compared to non-hybrid composite box results [9]. Kim et al. have investigated the crashworthiness of the aluminium crash box with different basic cross-section profile such as rectangular, hexagonal and octagonal shapes. It was concluded that the hexagonal cross-section shape could absorb higher energy capacity and mean crushing load [3].

In previous studies, several researchers have investigated the crashworthiness characteristics of hybrid tubular structures, which were fabricated using the filament winding technique [10–15]. Various researchers have explored the axial crushing behavior and crashworthiness characteristics of hybrid tubes by considering several factors such as loading conditions [16,17], geometry and

\* Corresponding author.

E-mail address: [neromaquanjin@gmail.com](mailto:neromaquanjin@gmail.com) (M. Quanjin).

cross-section shape [8,18–23]. However, as far as authors are aware, little work has been carried out to study crushing behaviour, compressive and tensile properties of the automotive crash box made of hybrid carbon/aramid material, and which are fabricated using hand lay-up method. To bridge the research gap, compressive properties and crushing behaviour of square hybrid carbon/aramid tube applied as the crash box was explored in detail under quasi-static axial compressive and tensile tests.

The structure of this paper is organized as follows. (i) Introduction: several related studies of the crash box have been reviewed and discussed. (ii) Material and methods: material preparation, quasi-static axial compressive and tensile experimental setups are mentioned in detail. (iii) Results and discussion: the main findings of quasi-static axial compressive and tensile tests are analyzed and discussed. (iv) Conclusion: the results of compressive and tensile properties of hybrid carbon/aramid material were studied and summarized.

## 2. Materials and methods

### 2.1. Material preparation

The resin, D.E.R.<sup>TM</sup> 331<sup>TM</sup> liquid epoxy resin was obtained from Salju Bistari Sdn. Bhd. The hardener, a modified cycloaliphatic amine JOINTMINE 905-3S was supplied by Epochemie International Pte Ltd, respectively. Typical properties of the epoxy and the hardener are selectively shown in Table 1. Physical properties of hybrid carbon/aramid weave laminates are briefly shown in Fig. 1. Hybrid carbon/aramid plain weave 3 K laminates are provided from Mitsubishi Rayon Co., Ltd. Table 2 exhibits the specification of the hybrid carbon/aramid weave 3 K laminates, which used 2/2 twill weave pattern of hybrid carbon/aramid laminates. 3 K means one bundle has 3000 fiber filaments, which has no relationship with the quality of the laminate sheet.

### 2.2. Fabrication procedure

Square hybrid carbon/aramid tubes were fabricated using hand layup method. The orientation of the hybrid laminates with 2/2 twill weave pattern has to be maintained in order to make sure that the fiber orientation remains uniformly on the entire wooden

**Table 1**  
Typical properties of the hardener and epoxy resin.

Specifications	Epoxy resin	Hardener
Type	D.E.R. <sup>TM</sup> 331 <sup>TM</sup>	JOINTMINE 905-3S
Color	<2	<3
Density (g/cm <sup>3</sup> )	1.16	–
Compressive strength (MPa)	112	98
Tensile strength (MPa)	79	68
Elongation at break (%)	4.4	–

**Table 2**  
Specifications of hybrid carbon/aramid weave laminate.

Specifications	Hybrid carbon/aramid laminate
Width (mm)	1200
Weight (g/m <sup>2</sup> )	210
Thickness (mm)	0.3
Ends (mm)	65
Picks (mm)	65
Warp fibre	(Pyrofil TR30S3K)/1
Weft fibre	(Pyrofil TR30S3K)/1 (Kevlar <sup>®</sup> 49)
Weave type	2/2 twill

crash box mold. The fiber orientation should be realigned as regularly as possible. The square hybrid carbon/aramid tube was prepared with 7 layers, which were mixed at a ratio of 2:1 with the epoxy and the hardener. The impregnated hybrid material was placed on the square wooden mold while a plastic roller was used to remove the extra resin and reduce the bubble. The specimen was fixed on the mandrel with two square holders by using the portable 3-axis filament winding machine [13,24]. The curing process took 2 h with 10 rpm rotation speed and cured for 24 h at room temperature. Fabrication procedure of square hybrid carbon/aramid tubes is shown in Fig. 2, involving preparation condition, fabrication method, and final specimen structure. Table 3 summarizes the geometric dimensions of all the specimens for the experimental study.

The hybrid carbon/aramid specimens for the tensile test were fabricated using hand layup method. The three layers were fabricated on a flat aluminium plate while mixing the epoxy and hardener with a ratio of 2:1. The plastic roller was used to distribute the resin mixture evenly. Three layers of specimens were initially prepared and completed. During the curing process, the hydraulic press machine was used to press two flat aluminium plates for 12 h at room temperature in order to obtain a better final specimen condition. When the specimen was fully cured, it was removed from the two flat aluminium plates. The specimen structure of the tensile test was cut using a hack saw according to the ASTM3039 standards, and the edges were trimmed and smoothed using a bench grinder. The specimen fabrication procedure of the tensile test is presented in Fig. 3, where fabrication process details are shown as follows. The geometric dimensions of specimens on the tensile test is summarized in Table 4.

### 2.3. Quasi-static compression test

The quasi-static compression test was conducted using the Instron 600dx universal testing machine, which provides a maximum capacity of 600 kN. Three specimens were used to perform the quasi-static compression test. The specimen was placed between the two compressive platens, and the axial direction of the specimen is oriented perpendicular to the compression platen. The crosshead speed of compression test was set as 2 mm/minute.

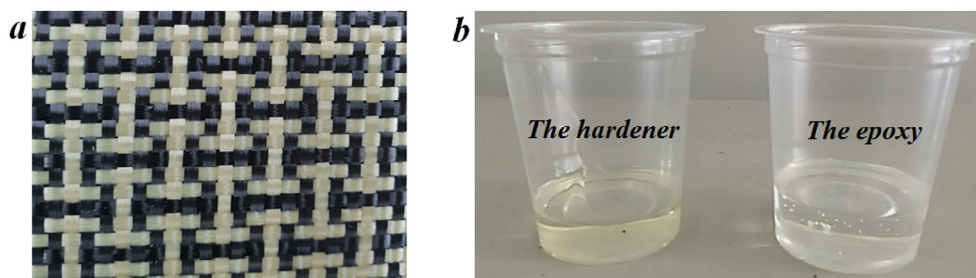


**Fig. 1.** Material preparation: (a) hybrid carbon/aramid weave laminate with 2/2 twill pattern; (b) the hardener and epoxy resin.

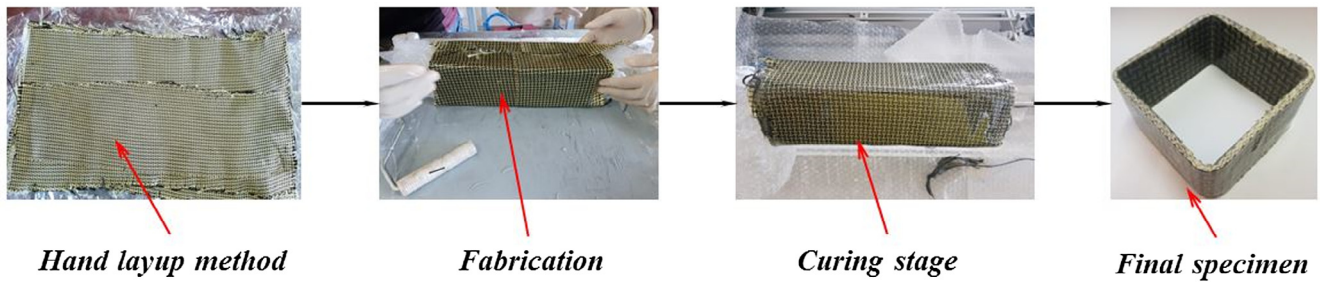


Fig. 2. Fabrication procedure of square hybrid composite carbon/aramid tube.

Table 3

Summary of three specimens for the quasi-static axial compression test.

Specimen ID	Height (mm)	Length (mm)	Width (mm)	Mass (g)	Stacking layers
Specimen 1	51.08	89.00	89.00	82	7
Specimen 2	49.37	85.60	85.30	77	7
Specimen 3	49.60	88.10	88.10	81	7
Average value	50.01	87.56	87.46	80	7

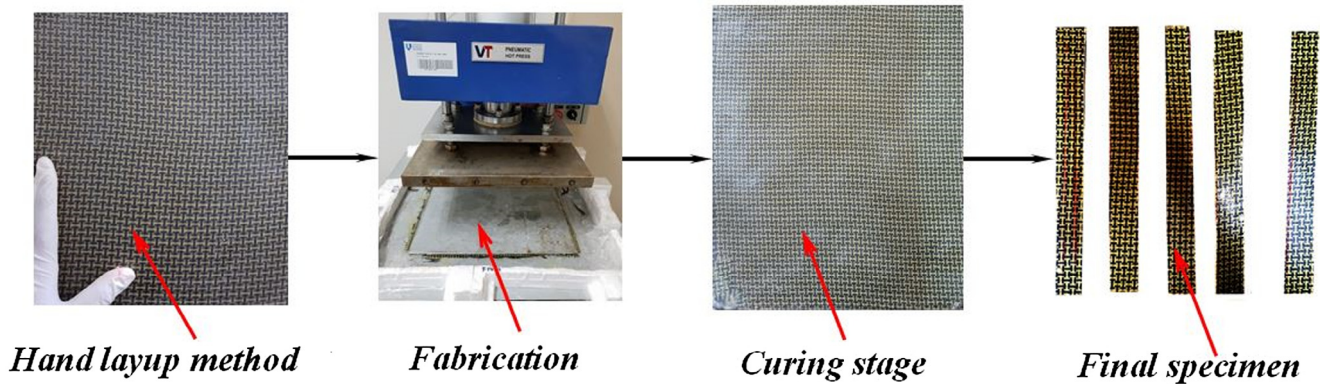


Fig. 3. Fabrication procedure of the tensile test.

Table 4

Summary of three specimens for the tensile test.

Specimen ID	Length (mm)	Width (mm)	Thickness (mm)	Stacking layers
Specimen 4	252	24.8	0.93	3
Specimen 5	248	25.3	0.92	3
Specimen 6	251	24.6	0.93	3
Average value	250	24.9	0.92	3

The compression displacement was 70% of the height of the square hybrid tube, which was 35 mm displacement from the start point to the end point. From the quasi-static axial compression test, compressive behaviour and failure mode of the hybrid tube were identified, such as compression modulus, energy absorption ( $EA$ ) and specific energy absorption ( $SEA$ ). Fig. 4 shows the quasi-static axial compression experiment setup, which presented the equipment setup (a) and quasi-static compression test condition (b).

Based on similar studies on the crushing behaviour of different tubular structures [20,25–27], several parameters have been used to evaluate the energy-absorbing characteristics, such as energy absorption ( $EA$ ) and specific energy absorption ( $SEA$ ).  $EA$  is represented the total energy absorbed during compression loading, which is calculated as

$$EA = \int_0^d F(x) dx \quad (1)$$

The specific energy absorption ( $SEA$ ) is defined as the energy absorption by per unit mass, as

$$SEA = \frac{EA}{m} \quad (2)$$

#### 2.4. Tensile test

To better understand the mechanical properties of hybrid carbon/aramid laminates, the tensile test was investigated in this study. The tensile test was performed using the Instron 3369 universal testing machine, which provided a maximum capacity of



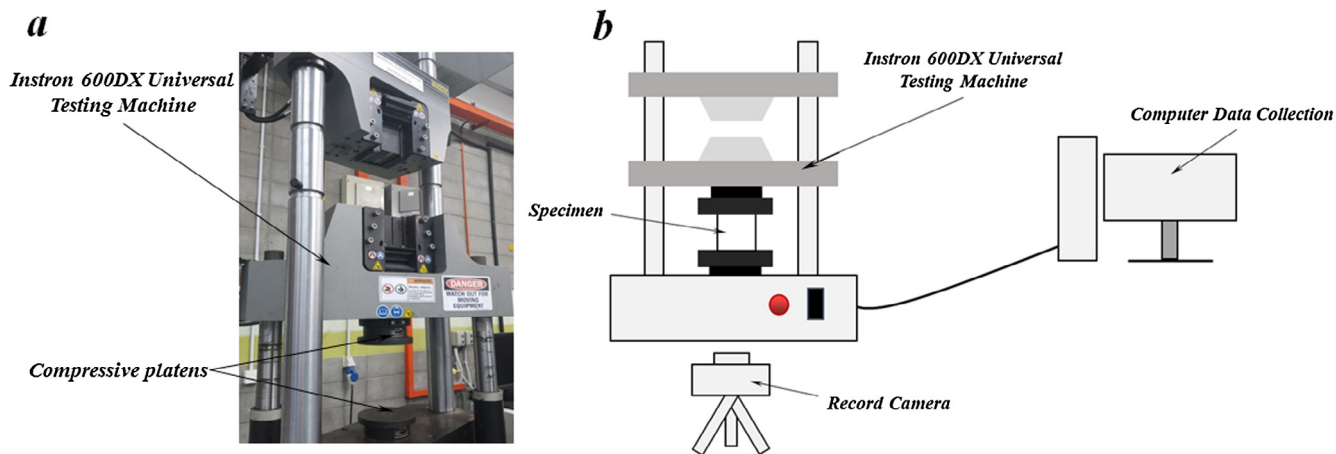


Fig. 4. Experimental procedure: (a) equipment overview; (b) quasi-static axial compression test setup.

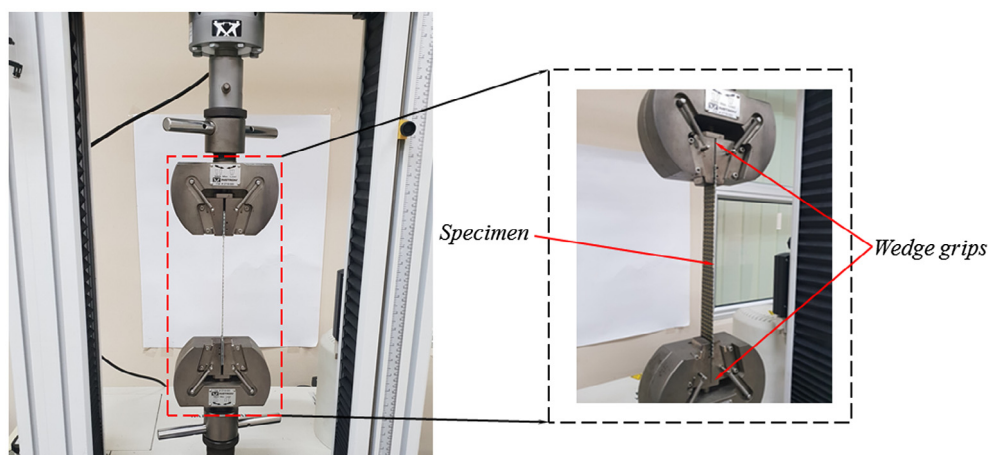


Fig. 5. Experimental procedure of hybrid carbon/aramid specimen in tensile test.

50 kN. The tensile test was performed with 2 mm/minute according to ASTM D3039 standards, and three specimens were tested in the same loading condition. The wedge grips were strongly tied between the specimen and clamp surfaces. Fig. 5 presents the experimental setup of the tensile test of the hybrid carbon/aramid specimen. The tensile test was used to evaluate the mechanical strength and stiffness properties of hybrid carbon/aramid laminates.

### 3. Results and discussion

Results of quasi-static axial compressive and tensile tests were presented and discussed. The collected data were adequately studied, analyzed, and evaluated, which involved compressive and tensile properties of hybrid carbon/aramid material.

#### 3.1. Result of quasi-static compressive test

The load versus displacement graphs obtained from the quasi-static axial compressive test, which presents a consistent pattern for all three specimens. The load versus displacement pattern can briefly be divided into two stages, which are elastic deformation stage and progressive deformation stage. In the elastic stage, the crushing force sharply increased in a steep manner until it

researched the peak force value. When the square hybrid specimens underwent elastic deformation, failure crushing and some buckling sound could be heard. During the initial progressive deformation stage, the matrix cracking and laminate bending started to occur at the top, bottom, or middle of the square structure. The square hollow specimen then collapsed, and the crushing load steadily dropped steadily rather than abruptly to a relatively lower level. For instance, the example crushing behaviour of one of the square hollow hybrid carbon/aramid tube under quasi-static axial compressive test is shown in Fig. 6.

Interestingly, there is no evidence of any sort of shearing failure as the crushing load progresses in the compressive test. The hybrid carbon/aramid tubes only became more and more compact as the compressive load progressed. This condition happened consistently for all three specimens during the quasi-static axial compressive test. Several studies had been carried out previously on the compressive test of crash box, which showed a quite similar pattern of the load versus displacement graphs [27,28]. The load versus displacement and strain versus strain curves of three specimens were shown in Fig. 7(a) and (b), which exhibited fairly the same trends in the quasi-static loading condition. The load versus displacement curve of specimen 1 displayed a higher load value in the progressive deformation stage except that the load abruptly dropped to a lower level at the displacement of around 20 mm, probably caused by much matrix or unstable compressive condi-

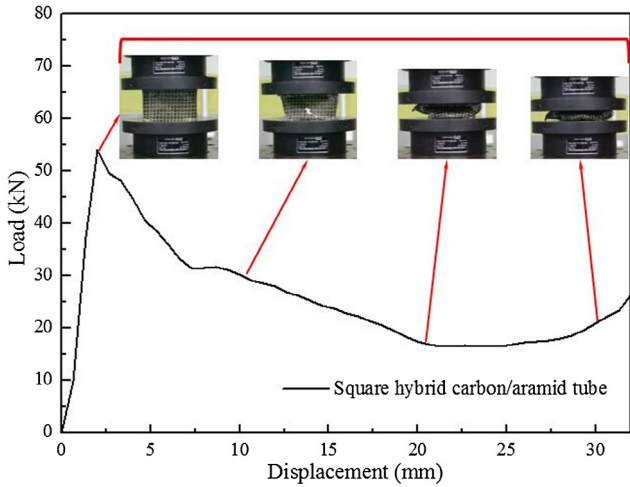


Fig. 6. The example crushing behaviour of square hybrid carbon/aramid tube on a quasi-static axial compressive test.

tion between two compressive platens and contacting surface of the specimen. Moreover, there can be quite different when it referred to the decreased extent under progressive deformation after it achieved peak load value.

The energy absorption capability of the hybrid carbon/aramid material was investigated and calculated according to the load versus displacement curve, which was used to evaluate compressive properties using this hybrid material under impacted condition. In this study, compressive properties such as energy absorption (EA), specific energy absorption (SEA), peak load, compressive modulus, and maximum stress were discussed and analyzed. Based on the crushing performance of the hybrid carbon/aramid beams,

related compressive properties were collected and summarized in Table 5. It was concluded that the hybrid carbon/aramid tube could provide a good compressive properties such as average 57.94 J of energy absorption (EA), average 0.72 kJ/kg of specific energy absorption (SEA), average 62.46 kN of crushing peak load, average 748.41 MPa of compressive modulus and average 36.29 MPa of maximum stress. Based on the findings of the compressive properties of hybrid carbon/aramid material, it exhibited that hybrid material has great potential to apply in automotive application as a lightweight crash box.

Fig. 8 presented the crushing failure mode of square hybrid carbon/aramid tubes after the quasi-static axial compressive test. Based on three of the final square hybrid carbon/aramid tubes, it occurred that delamination with multi-layers of specimens appeared on the top view. Moreover, it happened lamina bending on the final failure condition of specimens on the front and side views. The subsequent of the lamina bending failure mode had a series of quite subtle matrix cracks, which did not find hybrid fiber cracks. Matrix cracks and hybrid fiber bending occurred on the same consistent spots of the specimen, which mainly found in the lamina bending areas.

Fig. 9(a) compared the maximum load versus equivalent density of the experimental data investigated in quasi-static axial compression test with other commercial materials, including aluminium 7003, 7005, 6001 and 1050H14 types for crash box application [26,29]. It was found clear gap between the hybrid carbon/aramid material and other aluminium types. The equivalent density of the hybrid carbon/aramid material is less than 1/3 of other common aluminium material. It was concluded that hybrid composite material had a great potential to reduce weight for crash box applications in the automotive engineering.

Fig. 9(b) showed compressive stress versus equivalent density with several current materials. It was found that the hybrid carbon/aramid composite crash box was able to withstand almost

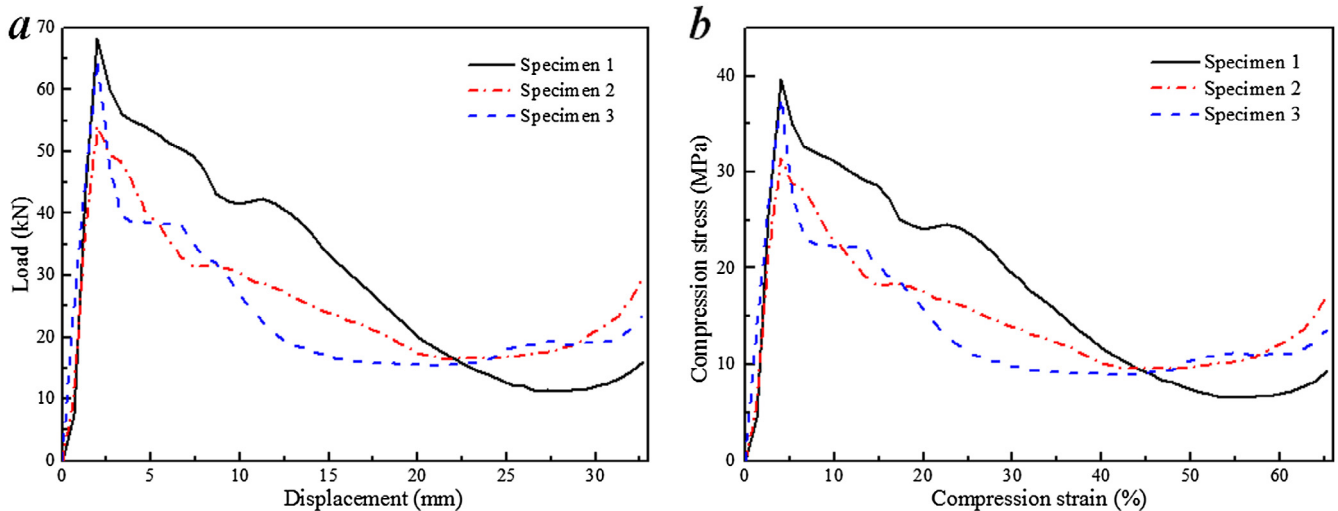


Fig. 7. Results of square hybrid carbon/aramid tubes under a quasi-static compression loading: (a) load versus displacement; (b) stress versus strain.

Table 5  
Summary of crashworthiness indicators of square hybrid carbon/aramid tubes.

Specimen ID	EA (J)	SEA (kJ/kg)	$F_{peak}$ (kN)	Compressive modulus (MPa)	Maximum compressive stress (MPa)
Specimen 1	58.00	0.70	68.40	510.79	39.74
Specimen 2	55.06	0.71	54.10	791.94	31.44
Specimen 3	60.77	0.75	64.88	942.50	37.70
Average value	57.94	0.72	62.46	748.41	36.29

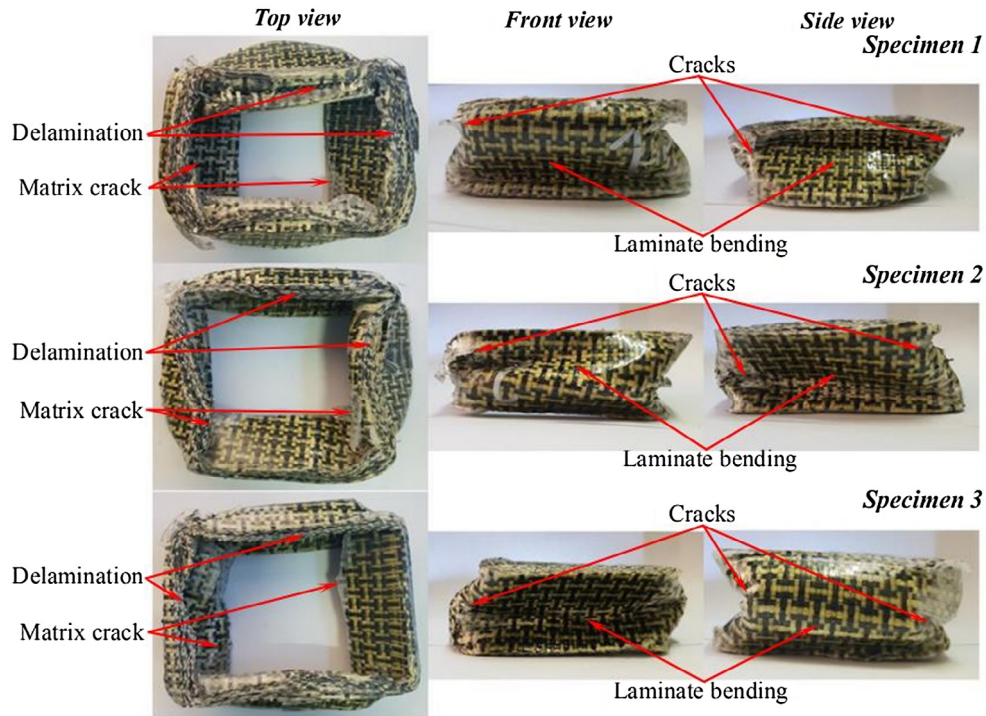


Fig. 8. Failure behaviour of square hybrid carbon/aramid tubes after quasi-static axial compressive test.

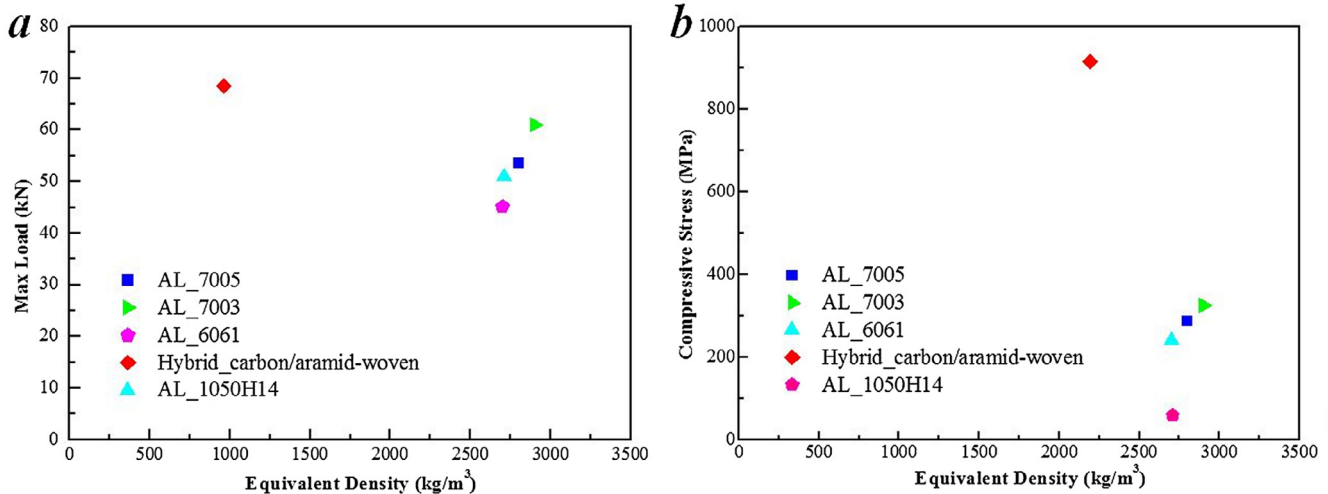


Fig. 9. Comparison result with current materials for crash box application: (a) maximum load versus equivalent density; (b) compressive stress versus equivalent density [23,24].

three times than the conventional aluminium counterpart. In terms of equivalent density perspective, the hybrid carbon/aramid composite crash box provided the lowest value of 2193 kg/m<sup>3</sup>, which exhibited that hybrid material can provide almost three times compressive stress with less weight cost in crash box application compared with commercial material. It was found that hybrid carbon/aramid material can achieve the highest compressive load and compressive stress values, which reduced the overall weight parameter without decreasing several compressive properties.

### 3.2. Result of tensile test

Based on the tensile test, the load versus displacement and strain versus stress curves were obtained to study tensile properties, which were presented in Fig. 10(a) and (b), respectively. The values of tensile modulus were obtained 7.70 GPa, 6.74 GPa and 7.10 GPa of specimen 4, 5 and 6 respectively. The ultimate tensile strength of specimens was obtained, which were 0.31 GPa, 0.26 GPa, and 0.25 GPa. It was found that hybrid carbon/aramid composite crash box provided better tensile properties such as

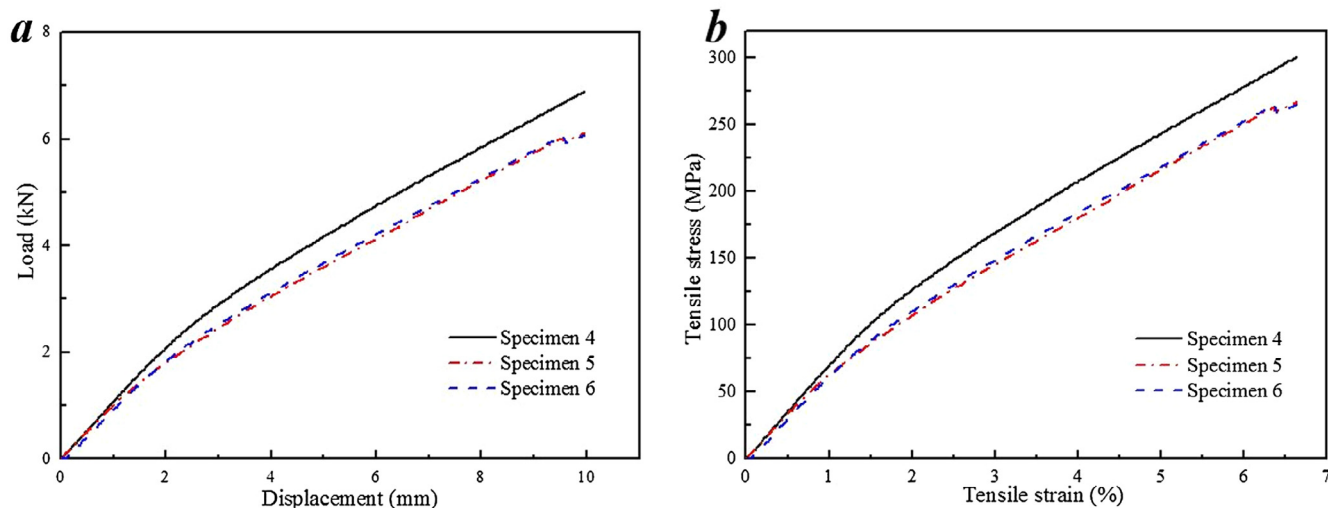


Fig. 10. Results of hybrid carbon/aramid specimen under tensile test: (a) load versus displacement; (b) stress versus strain.

Table 6

Summary of hybrid carbon/aramid specimens under tensile test.

Specimen ID	Tensile modulus (GPa)	Ultimate tensile strength (GPa)	Tensile stress at breaking point (GPa)
Specimen 4	7.70	0.31	0.11
Specimen 5	6.74	0.26	0.09
Specimen 6	7.10	0.25	0.10
Average value	7.18	0.27	0.10

an average 7.18 GPa of tensile modulus, an average 0.27 GPa of ultimate tensile strength, average 0.10 GPa of tensile stress. From comparison performance perspective, the ultimate tensile strength of aluminium material was only 0.11 GPa, and it highlighted that the hybrid carbon/aramid material showed almost 2.45 times higher than aluminium material [30]. Moreover, the summary of compressive properties of hybrid carbon/aramid specimen under tensile test were summarized in Table 6.

#### 4. Conclusion

The compressive properties of square hybrid carbon/aramid tubes and tensile properties of hybrid carbon/aramid material were investigated using the experimental method. The crushing behaviour, load versus displacement, and stress versus strain curves were explored through quasi-static axial compressive and tensile tests. The main conclusions are summarized as follows:

1. It is concluded that square hybrid carbon/aramid tubes provide average 57.94 J of energy absorption, an average 0.72 kJ/kg of specific energy absorption, average 62.46 kN of crushing peak load, average 748.41 MPa of compressive modulus and average 36.29 MPa of maximum stress. It highlights that hybrid carbon/aramid material provides the highest compressive load and compressive stress values compared to commercial material used in crash box application, which has great potential to use hybrid composite material to replace common materials in the automotive engineering.
2. The failure type of square hybrid carbon/aramid tubes is delamination, matrix cracking, and laminate bending as progressive deformation under a quasi-static axial compressive test.

#### Declaration of Competing Interest

The authors declare that they have no known competing financial interests or personal relationships that could have appeared to influence the work reported in this paper.

#### Acknowledgement

The authors are grateful to the Ministry of Education Malaysia: FRGS/1/2019/TK03/UMP/02/10. The research work is strongly supported by the Structural Materials & Degradation (SMD) Focus Group, Faculty of Mechanical and Automotive Engineering Technology, University Malaysia Pahang.

#### References

- [1] H. Zarei, M. Kröger, Optimization of the foam-filled aluminum tubes for crush box application, *Thin-Walled Struct.* 46 (2) (2008) 214–221.
- [2] M. Shin, S. Yi, O. Kwon, G. Park, Structural optimization of the automobile frontal structure for pedestrian protection and the low-speed impact test, *Proc. Inst. Mech. Eng. D: J. Automob. Eng.* 222 (12) (2008) 2373–2387.
- [3] S.B. Kim, H. Huh, G. Lee, J. Yoo, M. Lee, Design of the cross section shape of an aluminum crash box for crashworthiness enhancement of a car, *Int. J. Mod. Phys. B* 22 (31n32) (2008) 5578–5583.
- [4] H. Ghasemnejad, B. Blackman, H. Hadavinia, B. Sudall, Experimental studies on fracture characterisation and energy absorption of GFRP composite box structures, *Compos. Struct.* 88 (2) (2009) 253–261.
- [5] M.D. Iozsa, D. Micu, G. Frăţilă, F. Antonache, Influence of Crash Box on Automotive Crashworthiness. *Recent Advances in Civil Engineering and Mechanics*, ISBN.978-60.
- [6] Z. Bai, K. Sun, F. Zhu, L. Cao, J. Hu, C.C. Chou, et al., Crashworthiness optimal design of a new extruded octagonal multi-cell tube under dynamic axial impact, *Int. J. Veh. Saf.* 10 (1) (2018) 40–57.
- [7] J. Obradovic, S. Boria, G. Belingardi, Lightweight design and crash analysis of composite frontal impact energy absorbing structures, *Compos. Struct.* 94 (2) (2012) 423–430.
- [8] H. Zarei, M. Kröger, H. Albertsen, An experimental and numerical crashworthiness investigation of thermoplastic composite crash boxes, *Compos. Struct.* 85 (3) (2008) 245–257.
- [9] H. Ghasemnejad, H. Hadavinia, A. Aboutorabi, Effect of delamination failure in crashworthiness analysis of hybrid composite box structures, *Mater. Des.* 31 (3) (2010) 1105–1116.
- [10] H. El-Hage, P. Mallick, N. Zamani, Numerical modelling of quasi-static axial crush of square aluminium-composite hybrid tubes, *Int. J. Crashworthiness* 9 (6) (2004) 653–664.
- [11] J. Bouchet, E. Jacquelin, P. Hamelin, Dynamic axial crushing of combined composite aluminium tube: the role of both reinforcement and surface treatments, *Compos. Struct.* 56 (1) (2002) 87–96.
- [12] J. Babbage, P. Mallick, Static axial crush performance of unfilled and foam-filled aluminum-composite hybrid tubes, *Compos. Struct.* 70 (2) (2005) 177–184.



- [13] M. Quanjin, M. Rejab, N.M. Kumar, M. Idris, Experimental assessment of the 3-axis filament winding machine performance, *Results Eng.* (2019) 100017.
- [14] M. Quanjin, M. Rejab, J. Kaige, M. Idris, M. Harith, Filament winding technique, experiment and simulation analysis on tubular structure, *IOP Conf. Ser. Mater. Sci. Eng.* IOP Publ. (2018) 012029.
- [15] M. Quanjin, M. Rejab, M. Idris, B. Zhang, M. Merzuki, N.M. Kumar, Wireless technology applied in 3-axis filament winding machine control system using MIT app inventor, *IOP Conf. Series: Mater. Sci. Eng.* IOP Publ. (2019) 012030.
- [16] A.P. Kumar, M.S. Sundaram, An axial crushing characteristics of hybrid kenaf/glass fabric wrapped aluminium capped tubes under static loading, *Int. J. Mech. Prod. Eng. Res. Dev.* 8 (6) (2018) 201–206.
- [17] A.P. Kumar, Quasi-static crushing behaviour of axially compressed combined aluminium-composite tubes, *Int. J. Mech. Eng. Technol.* 9 (8) (2018) 907–914.
- [18] R.M. Lima, Z. Ismarrubie, E. Zainudin, S. Tang, Effect of length on crashworthiness parameters and failure modes of steel and hybrid tube made by steel and GFRP under low velocity impact, *Int. J. Crashworthiness* 17 (3) (2012) 319–325.
- [19] H. Zarei, M. Kröger, Crashworthiness optimization of empty and filled aluminum crash boxes, *Int. J. Crashworthiness* 12 (3) (2007) 255–264.
- [20] M. Guden, S. Yüksel, A. Taşdemirci, M. Tanoğlu, Effect of aluminum closed-cell foam filling on the quasi-static axial crush performance of glass fiber reinforced polyester composite and aluminum/composite hybrid tubes, *Compos. Struct.* 81 (4) (2007) 480–490.
- [21] H.-W. Song, Z.-M. Wan, Z.-M. Xie, X.-W. Du, Axial impact behavior and energy absorption efficiency of composite wrapped metal tubes, *Int. J. Impact Eng.* 24 (4) (2000) 385–401.
- [22] M. Mirzaei, M. Shakeri, M. Sadighi, H. Akbarshahi, Experimental and analytical assessment of axial crushing of circular hybrid tubes under quasi-static load, *Compos. Struct.* 94 (6) (2012) 1959–1966.
- [23] Praveen Kumar A. Experimental analysis on the axial crushing and energy absorption characteristics of novel hybrid aluminium/composite-capped cylindrical tubular structures. *Proceedings of the Institution of Mechanical Engineers, Part L: Journal of Materials: Design and Applications.* 2019:1464420719843157.
- [24] M. Quanjin, M. Rejab, I. Sahat, M. Amiruddin, D. Bachtar, J. Siregar, et al., Design of portable 3-axis filament winding machine with inexpensive control system, *J. Mech. Eng. Sci.* 12 (1) (2018) 3479–3493.
- [25] M. Quanjin, M. Sahat, M.R. Mat Rejab, S. Abu Hassan, B. Zhang, M.N. Merzuki, The energy-absorbing characteristics of filament wound hybrid carbon fiber-reinforced plastic/polylactic acid tubes with different infill pattern structures, *J. Reinforced Plast. Compos.* 38 (2019) 1067–1088.
- [26] B. Simhachalam, K. Srinivas, C.L. Rao, Energy absorption characteristics of aluminium alloy AA7XXX and AA6061 tubes subjected to static and dynamic axial load, *Int. J. Crashworthiness* 19 (2) (2014) 139–152.
- [27] H. Jiang, Y. Ren, B. Gao, J. Xiang, F.-G. Yuan, Design of novel plug-type triggers for composite square tubes: enhancement of energy-absorption capacity and inducing failure mechanisms, *Int. J. Mech. Sci.* 131 (2017) 113–136.
- [28] D. Siromani, G. Henderson, D. Mikita, K. Mirarchi, R. Park, J. Smolko, et al., An experimental study on the effect of failure trigger mechanisms on the energy absorption capability of CFRP tubes under axial compression, *Compos. A Appl. Sci. Manuf.* 64 (2014) 25–35.
- [29] A.K. Toksoy, M. Guden, Partial Al foam filling of commercial 1050H14 Al crash boxes: the effect of box column thickness and foam relative density on energy absorption, *Thin-walled Struct.* 48 (7) (2010) 482–494.
- [30] P.T. Summers, Y. Chen, C.M. Rippe, B. Allen, A.P. Mouritz, S.W. Case, et al., Overview of aluminum alloy mechanical properties during and after fires, *Fire Sci. Rev.* 4 (1) (2015) 3.